




Magnetostratigraphic evidence for deep-sea erosion on the Pacific Plate, south of Mariana Trench, since the middle Pleistocene: potential constraints for Antarctic bottom water circulation

Xiguang Deng, Liang Yi, Greig A. Paterson, Huafeng Qin, Haifeng Wang, Huiqiang Yao, Jiangbo Ren, Junyi Ge, Hongzhou Xu, Chenglong Deng & Rixiang Zhu


To cite this article: Xiguang Deng, Liang Yi, Greig A. Paterson, Huafeng Qin, Haifeng Wang, Huiqiang Yao, Jiangbo Ren, Junyi Ge, Hongzhou Xu, Chenglong Deng & Rixiang Zhu (2016) Magnetostratigraphic evidence for deep-sea erosion on the Pacific Plate, south of Mariana Trench, since the middle Pleistocene: potential constraints for Antarctic bottom water circulation, International Geology Review, 58:1, 49-57, DOI: [10.1080/00206814.2015.1055597](https://doi.org/10.1080/00206814.2015.1055597)

To link to this article: <http://dx.doi.org/10.1080/00206814.2015.1055597>

 View supplementary material 

 Published online: 29 Jun 2015.

 Submit your article to this journal 

 Article views: 23

 View related articles 

 View Crossmark data 

Magnetostratigraphic evidence for deep-sea erosion on the Pacific Plate, south of Mariana Trench, since the middle Pleistocene: potential constraints for Antarctic bottom water circulation

Xiguang Deng^a, Liang Yi^{b,c}, Greig A. Paterson^d, Huafeng Qin^b, Haifeng Wang^a, Huiqiang Yao^a, Jiangbo Ren^a, Junyi Ge^e, Hongzhou Xu^c, Chenglong Deng^b and Rixiang Zhu^b

^aKey Laboratory of Marine Mineral Resources, Ministry of Land and Resources, Guangzhou Marine Geological Survey, Guangzhou, China; ^bState Key Laboratory of Lithospheric Evolution, Institute of Geology and Geophysics, Chinese Academy of Sciences, Beijing, China; ^cSanya Institute of Deep-sea Science and Engineering, Chinese Academy of Sciences, Sanya, China; ^dKey Laboratory of the Earth's Deep Interior, Institute of Geology and Geophysics, Chinese Academy of Sciences, Beijing, China; ^eKey Laboratory of Vertebrate Evolution and Human Origins, Institute of Vertebrate Palaeontology and Palaeoanthropology, Chinese Academy of Sciences, Beijing, China

ABSTRACT

The Antarctic Bottom Water (AABW) current plays a crucial role in storing and transporting heat, water, and nutrients around the world. However, it is impossible to monitor AABW in the Plio-Pleistocene by direct measurement. Hence, abyssal erosion was usually chosen as an effective indicator of the presence of the AABW in the Indian and Eastern Pacific Oceans during that period. Here, we report a high-resolution magnetostratigraphy of a gravity core, the JL7KGC-01A from the south of the Mariana Trench, northwest Pacific Ocean. The main results are as follows: (1) polarity data suggest that the sequence recorded the late Gauss chron to the early Brunhes chron, including the Jaramillo, Cobb Mountain, and Olduvai normal subchrons; (2) the sedimentary processes in the study area since 2.9 Ma show three stages of sedimentation: 83 cm/Ma during 2.9–1.2 Ma, 183 cm/Ma during 1.2–0.7 Ma, and no sedimentation since ~0.7 Ma; (3) the area south of the Mariana Trench experienced a significant change in the deposition rate at 1.2 Ma, which could be correlated with the intensified desertification in inland Asia, and experienced a prominent depositional hiatus since the early middle Pleistocene, which likely resulted from the enhanced/expanded AABW. Based on these new polarity data and comparisons with previous studies around the Pacific Ocean, we therefore propose that the AABW experienced a notable change during the early–mid Pleistocene transition.

ARTICLE HISTORY

Received 11 March 2015
Accepted 23 May 2015

KEYWORDS

Mariana Trench;
magnetostratigraphy;
Plio-Pleistocene; abyssal
erosion

Introduction

The ocean bottom waters are characterized by distinct oxygen content, salinity, temperature, and density, in comparison to upper layers, and play a major role in global transportation of heat and energy. Among the most important global bottom waters, the Antarctic Bottom Water (AABW) is the main source for bottom waters in the Southern Ocean, northwest Pacific Ocean, and Atlantic Ocean. The AABW plays an important role in global climate change by storing and transporting heat, freshwater, and carbon around the Earth, and has therefore attracted great scientific attention during the past decade (e.g. Johnson 2008; Marshall and Speer 2012; Ohshima *et al.* 2013). However, the bottom water flows so slowly that only a few proxies are effective in determining its character in the past (e.g. Jacobs *et al.* 1970; Whitworth and Orsi 2006; Gordon *et al.* 2009, 2010). As a consequence, there are significant gaps in our understanding of the AABW.

Deep-sea erosion, which was broadly reported in the Indian and eastern Pacific Oceans (e.g. Kennett and Watkins 1975; Huang and Watkins 1977; Watkins and Kennett 1977; Ledbetter and Ciesielski 1982; Keller and Barron 1983), has provided unique information about the presence, transportation, and intensity of the AABW. For instance, based on 187 cores from the southeast Indian Ocean, Watkins and Kennett (1977) reconstructed the spatial distribution of surface sediment age and reported widespread deep-sea erosion in response to high bottom-water velocity. In the eastern Pacific Ocean, previous work strongly suggested that the AABW migrated eastward and northward into the Clarion–Clipperton fracture zone (C–C zone) several times in the Cenozoic, which caused considerable erosion in this area (Barron and Keller 1982).

The Mariana Trench lies at the boundary between the eastern Philippine Sea Plate and the subducting

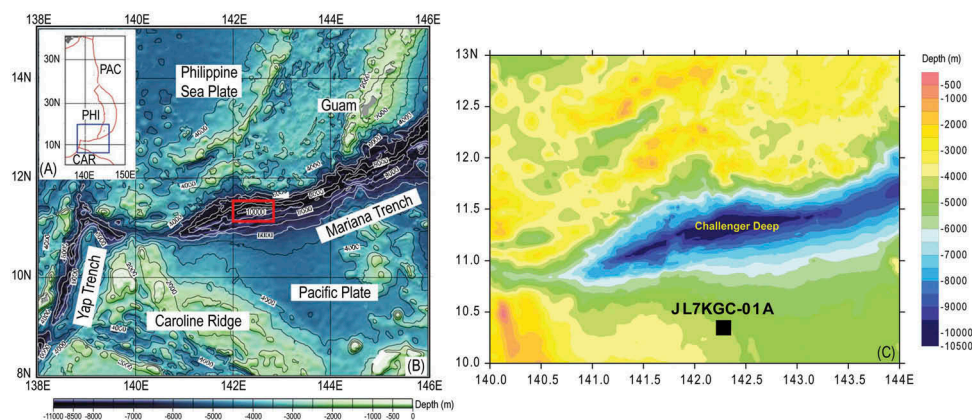


Figure 1. Tectonic position (A) and schematic map of the Mariana Trench region as well as the location of the JL7KGC-01A core (C). PAC, Pacific Plate; PHI, Philippine Sea Plate; and CAR, Caroline ridge. The bathymetric data of the Mariana Trench was generated using the open and free software DIVA-GIS 7.5 (<http://www.diva-gis.org/>). The magnetic inclination at the drilling site (142.28° E, 10.35° N) has two expectations: $3.46^{\circ} \pm 0.27^{\circ}$ and $7.23^{\circ} \pm 0.29^{\circ}$ according to the International Geomagnetic Reference Field (IGRF12) model (data covering 1590–2015 AD) (<http://www.ngdc.noaa.gov/geomag/>) (Supplemental data, Figure S5).

Pacific Plate (Figure 1A). The subduction along the boundary began in the Eocene prior to ~ 50 Ma (Jurdy 1979; Ranken *et al.* 1984). The trench is a non-accretionary convergent plate margin, wherein the basement of the overriding plate is in direct contact with the subducting plate at the trench axis and no material is accreted from the subducting plate (Hussong and Uyeda 1981). As a result, there is no significant infilling of the trench by accumulating sediments (Fryer *et al.* 2003), resulting in the deepest part of Earth's surface. The Mariana Trench is also a possible key path of the AABW (Talley *et al.* 2011), which can migrate northward and trigger the global thermohaline circulation in the Pacific (Supplemental data, Figure S4). Due to lack of evidence from this area, it is hard to know when the AABW migrated to the region and what the effects of such migration were. In this study, we investigate a gravity core collected from the Pacific Plate, at a locality south of the Mariana Trench, in 2012. We use magnetostratigraphy to reconstruct an age model for this core and assess the potential link between sedimentary history and abyssal processes and the presence of the AABW in this region during the late Plio-Pleistocene Epoch.

Material

The core, JL7KGC-01A, was collected in June 2012, using a gravity driller on the Pacific Plate, south of the Mariana Trench (Figure 1). The driller is 6 m long with a diameter of 7 cm. After coring from an area with a water depth of 4430 m, a 2.41 m-long sediment was obtained. About 3 cm-thick sediment from sediment top was fluid-like and collected for biological studies

on board. The 2.38 m-sediment core was then cut into three pieces and stored at an air temperature of 4°C . Due to water loss, pressure change, sediment loss in cutting, and/or other changes, the sediment shrank $\sim 1.5\%$ in length and finally 2.35 m-sediment was obtained after the cruise.

The sediment is homogenous carbonate-free muds with a median grain size of $6\text{--}12\ \mu\text{m}$. Its colour is dark brown (10YR 3/3) through the whole core with yellow spots (10YR 7/8). There are some micro-nodules with <1 mm diameter within 162–165 cm interval of the core (Figure 2). The sediment contains mineral, quartz grains and zeolite, and amphibole grains in minority. After the cruise, the JL7KGC-01A core was sampled at 2 cm interval using non-magnetic plastic cubes ($2 \times 2 \times 2\ \text{cm}^3$) and 115 specimens in total were collected for magnetic polarity study.

Methods

These 115 specimens from the JL7KGC-01A core were subjected to stepwise alternating field (AF) demagnetization up to a peak field of 80 mT (17 steps). The natural remanent magnetization of each specimen was measured using a three-axis cryogenic magnetometer (2G Enterprise, USA) installed in magnetically shielded room (residual fields $<300\ \text{nT}$).

Characteristic remanent magnetization (ChRM) directions were determined using principal component analysis (PCA, Kirschvink 1980) as implemented by the palaeomagnetism data analysis software (PGMSC, V4.2) developed by Randolph J. Enkin. The ChRM directions were fitted through the origin using at least four consecutive demagnetization steps and were only accepted

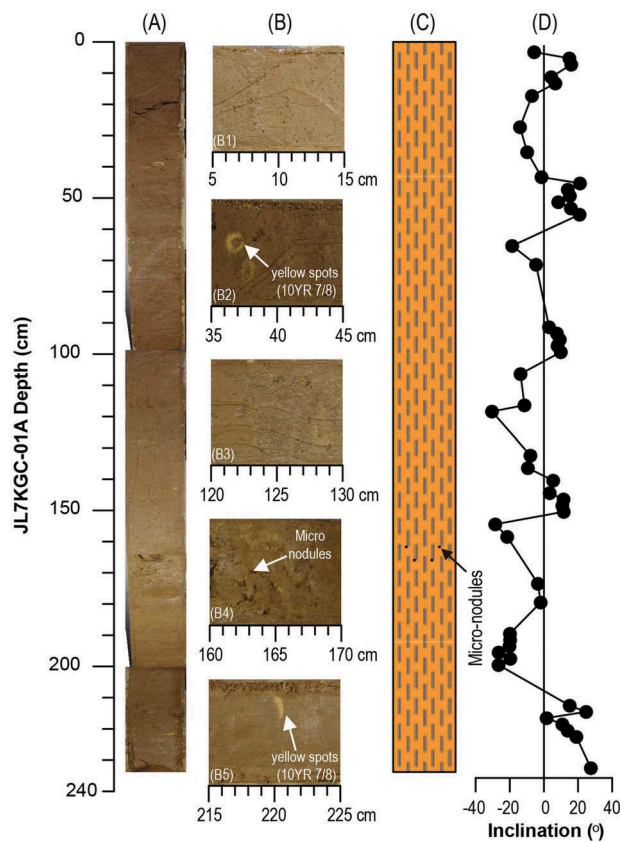


Figure 2. Photography (A) and some details (B1–B5), lithological changes (C), and magnetic inclinations (D) of the JL7KGC-01A core. The length of the core is 2.35 m, and its colour is dark brown (10YR 3/3) through the whole core with yellow spots (10YR 7/8). Some micro-nodules within 162–165 cm interval were observed. Please see details in the text.

if the maximum angular deviation (MAD) was less than 10° .

Rock magnetic measurements, which include isothermal remanent magnetization (IRM), IRM acquisition curves, hysteresis loops, and the associated ΔM and $d\Delta M/dB$ curves, were made on four representative specimens.

Hysteresis parameters were measured using a MicroMag 3900 vibrating sample magnetometer (VSM). The magnetic field was cycled between ± 1.5 T for each specimen. Saturation magnetization (M_s), saturation remanence (M_{rs}), and coercivity (B_c) were determined after the correction for the paramagnetic contribution identified from the slope at high fields. Specimens were then demagnetized in alternating fields up to 1.5 T, and an IRM was imparted from 0 to 1.5 T (IRM1.5 T, hereafter termed SIRM) also using the MicroMag 3900 VSM. Subsequently the SIRM was demagnetized in a stepwise backfield up to -0.4 T to obtain the coercivity of remanence (B_{cr}).

Results

Magnetic mineralogy

The sediments may consist of a mixture of different magnetic minerals with variable grain sizes or concentrations. Partitioning methods (e.g. Robertson and France 1994; Kruiver *et al.* 2001; Egli 2003) were used in order to analyse the magnetic composition. IRM acquisition curves of selected specimens were analysed by using the Matlab@ 7.1 programme, and the derivative curves were plotted to illustrate the coercivity distributions (Figure 3). The curves show a one-humped distribution, whose major coercivities are at 30–60 mT. This lower-coercivity predominant component is likely magnetite.

Hysteresis loops and ΔM and $d\Delta M/dB$ curves were used to further assess the magnetic mineralogy. All the selected specimens display pronounced superparamagnetic or pseudo-single domain behaviour (Figure 4), implying that the predominant magnetic mineral in the sediment is low-coercivity magnetite. The ΔM and $d\Delta M/dB$ curves, which are sensitive only to the remanence-carrying phases (e.g. Jackson *et al.* 1990; Tauxe *et al.* 1996; Tauxe 2010), were used to reveal the different coercivity spectra contained in the hysteresis loops. There is only one type of $d\Delta M/dB$ curve for the specimens studied and this is characterized by only one hump at 30–50 mT, indicating the presence of magnetite.

Therefore, all rock magnetic measurements are consistent with each other, and the dominant magnetic mineral in these sample sediments is magnetite.

Palaeomagnetic results

Demagnetization results of representative specimens are shown as orthogonal diagrams (Zijderveld 1967) (Figure 5). Generally, the stable ChRM component, which from the rock magnetic evidence is carried by magnetite, was isolated between 20 and 50 mT. A total of 49 specimens (~43%) gave reliable characteristic remanence directions under the criterion of four continuous AF points for calculation and an MAD value $\leq 10^\circ$ (Figure 2), and this number changes to 79 (~69%) and 92 (~80%) with the MAD $\leq 15^\circ$ and 20° , respectively. Because there is no significant difference between results in different criteria (Supplemental data, Figure S1), based on these 49 specimens with a more restricted criterion, we obtained nine polarity magnetozones (Figure 6): four of reverse polarity (R1–R4) and five of normal polarity (N1–N5). Given that no absolute declination data are available (Supplemental data,

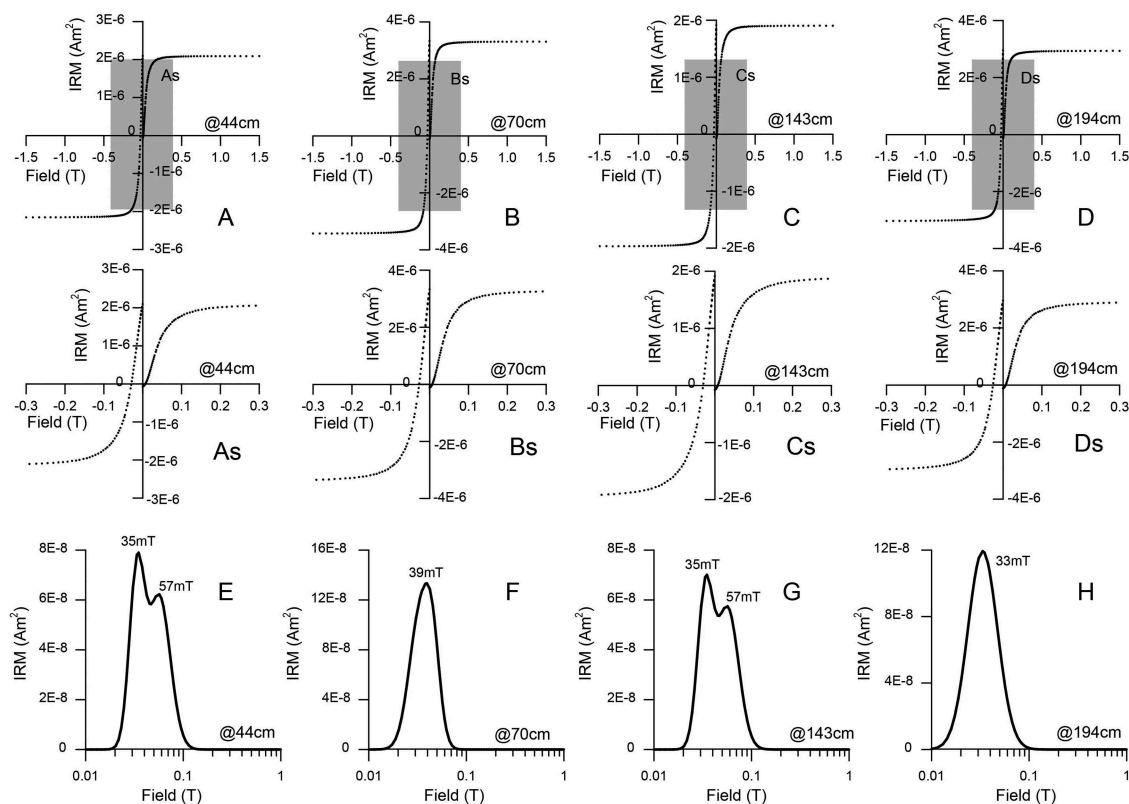


Figure 3. IRM acquisition curves (A–D are normal diagrams, and As–Ds are cut off at ± 0.3 T for reasons of clarity) and coercivity distributions (E–H) for selected specimens from the JL7KGC-01A core, which is calculated using the Matlab@ 7.1 program.

Figure S2), only the inclination data are used to define the magnetic polarity stratigraphy (Figure 5).

Discussion

Chronostratigraphic framework of the JL7KGC-01A core

Given that the sediment through the whole core is fairly homogeneous and there is no physical evidence indicating the presence of any considerable depositional hiatus, we therefore have to rely on identification of any hiatus through the age model. Nannofossil identification through the whole core was conducted at 10 cm intervals, before palaeomagnetic study. Most of the fossils were completely dissolved, but fortunately two partially dissolved species were identified: *Hemidiscus cuneiformis* at 10 cm and *Coscinodiscus nodulifer* at 100 cm (Figure 6). A regional nannofossil study in the southern Mariana Trench by a box sampler found that *Spongaster tetras* were dominant in the sediment (Deng XG, unpublished data). The presence of these nannofossils suggests that these sediments are late Pliocene to Pleistocene in age. The magnetostratigraphy for

JL7KGC-01A should thus be correlated with the chrons/subchrons of the late Plio-Pleistocene period.

Subsequently, we correlate the magnetozones determined from the JL7KGC-01A core to the geomagnetic polarity timescale (GPTS) of Ogg and Smith (2004) and Hilgen *et al.* (2012) (Figure 6). Magnetozones N1 and N5 correspond to the early part of the Brunhes chron and the late Gauss chron, respectively; magnetozones N2, N3, and N4 correspond to the Jaramillo, Cobb Mountain (Supplemental data, Figure S3), and Olduvai normal subchrons within the Matuyama reverse chron, respectively. The reversed magnetozones, R1–R4, correlate with the successive reverse polarity parts of the intervening Matuyama chron.

By integrating the magnetostratigraphic results and biochronologic constraints, a chronostratigraphic framework for the JL7KGC-01A core can be established. Due to the homogeneous sedimentation and no significant sedimentary boundary within the core, we prefer to set the transitions between normal and reverse magnetozones directly to the boundary of the magnetochrons (Ogg and Smith 2004; Hilgen *et al.* 2012). The depth-age model is shown in Figure 5 and indicates sedimentation rates that range from 80 to 180 cm/Ma for the JL7KGC-01A.

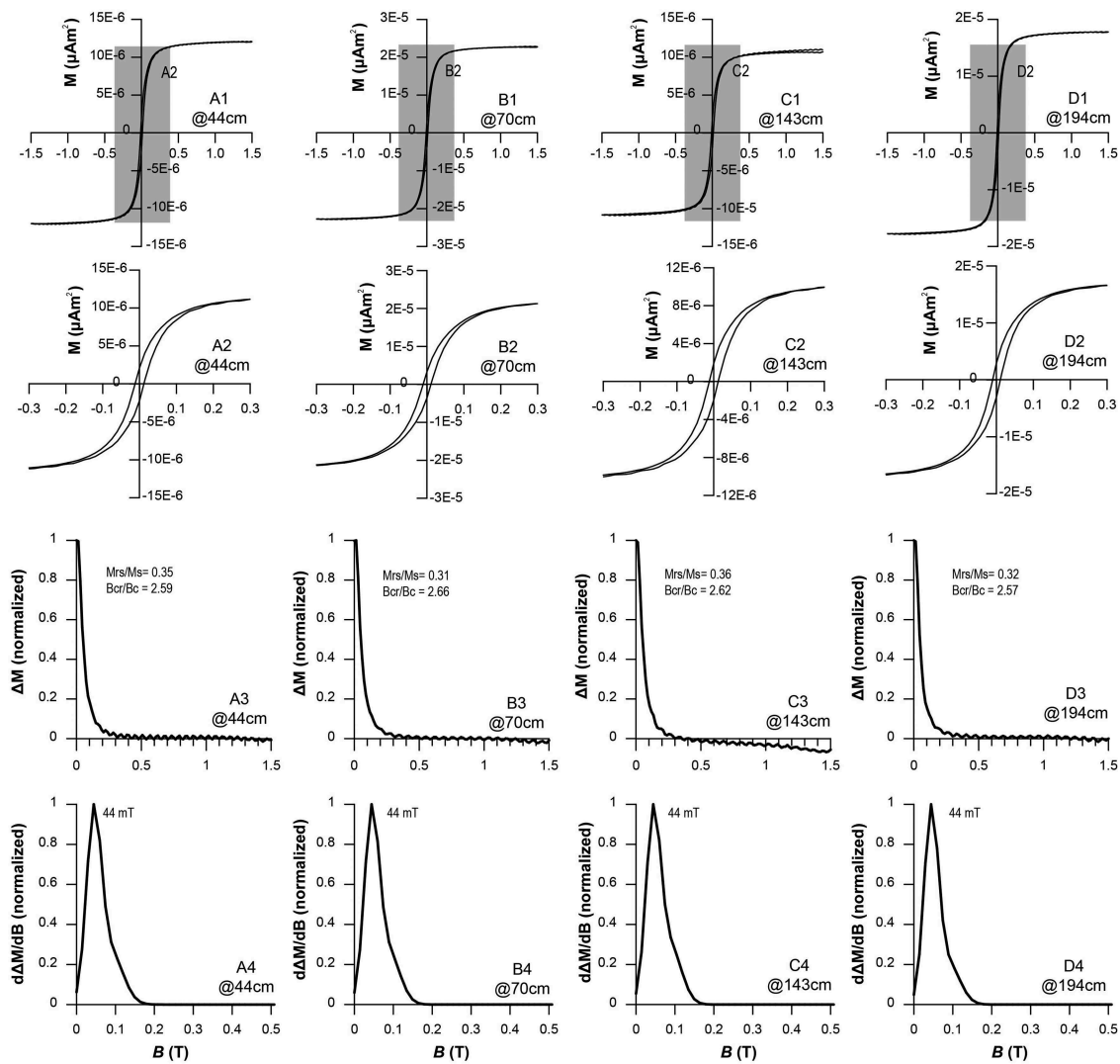


Figure 4. Hysteresis loops (A1–D1 are normal diagrams, and A2–D2 are cut off at ± 0.3 T for reasons of clarity) along with the ΔM curves (A3–D3) and $d\Delta M/dB$ curves (A4–D4) for selected specimens from the JL7KGC-01A core. The hysteresis loops were measured in fields up to ± 1.5 T. The numbers in figures A3–D3 represent the fields at which humps occur.

Sediment accumulation process since the late Pliocene

From our chronostratigraphic framework of the JL7KGC-01A core, we identify a distinct change in the sediment accumulation rate (SAR) from 83 ± 3 to 183 ± 15 cm/Ma across the termination of the Cobb Mountain normal subchron.

There are two possible mechanisms related to this large SAR transition: a change (1) in the sediment flux or (2) in the volume of the infilling basin.

The Mariana system is a non-accretionary convergent plate margin, in which no material is accreted from the subducting plate (Hussong and Uyeda 1981) and there is no significant infilling of the trench by accumulating sediments (Fryer *et al.* 2003). Given that the sediment in the northwest Pacific is dominantly from the inner Asian

continent (e.g. Rea 1994; Asahara *et al.* 1999; Greaves *et al.* 1999; Takebe 2005), the sediment in the study area can be correlated with aeolian input from inner Asia (Supplemental data, Figure S4). During the late Plio-Pleistocene period, according to the study by Sun and An (2005), the accumulation rate of aeolian deposits across the Chinese Loess Plateau increased with fluctuations since the late early Pleistocene with a notable increase during the time interval between 1.5 and 1.2 Ma. This rate jump was also reported by Sun and Liu (2000), in which the period with significantly increased aeolian SAR was recognized as 1.1–0.9 Ma. Therefore, this increase in SAR could be attributed to aridification of the Asian interior.

On the other hand, the Mariana Trench is the boundary between the eastern Philippine Sea Plate and the

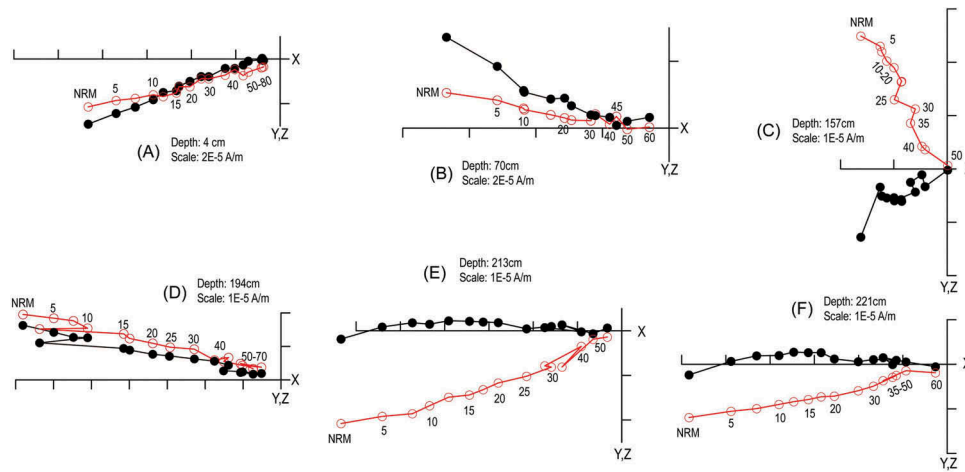


Figure 5. Orthogonal projections of progressive alternating field demagnetization for representative specimens. The solid (open) circles represent the horizontal (vertical) planes. The numbers in A–F refer to the alternating fields in mT. NRM is the natural remanent magnetization. Note that the magnetic declinations are arbitrary.

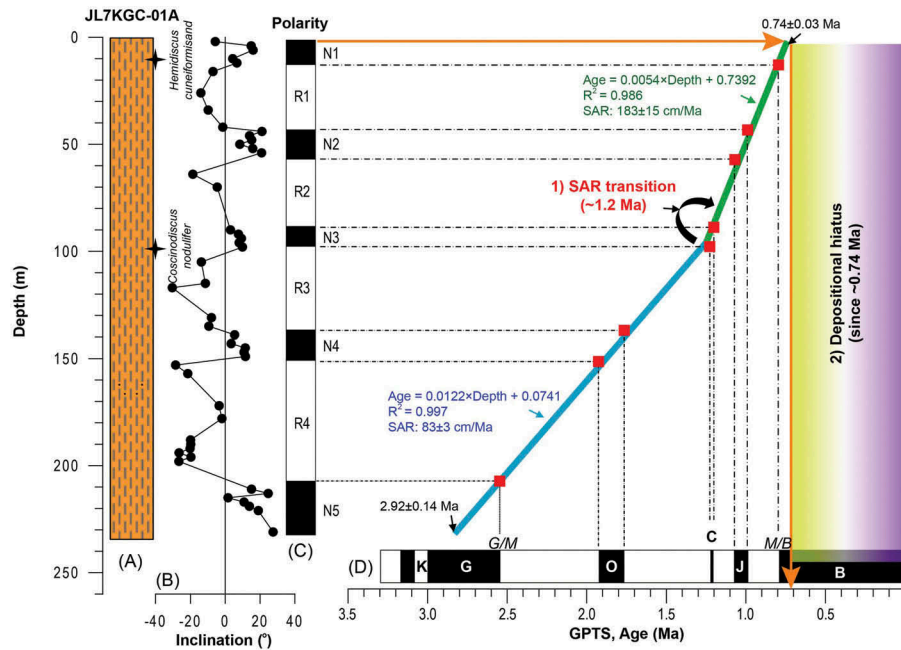


Figure 6. Lithology and nannofossils (A), magnetostratigraphy (B, C) and age–depth relationships for the JL7KGC-01A core. Dashed lines between (C) and (D) represent possible correlations of the recognized magnetozones (N1–N5 and R1–R4) to the geomagnetic polarity timescale (GPTS) (Ogg and Smith 2004; Hilgen *et al.* 2012). SAR, sediment accumulation rate. In (D), B, Brunhes; J, Jaramillo; C, Cobb Mountain; O, Olduvai; G, Gauss; M, Matuyama; K, Keana; G/M, Gauss–Matuyama boundary; M/B, Matuyama–Brunhes boundary. Two major findings ‘(1) SAR transition and (2) depositional hiatus’ are also labelled. See discussion in the text.

subducting Pacific Plate. As a consequence, the sediment infilling capacity is determined by the east–west collision between the Asian and North American plates. As an indicator, the Japan Alps ascended to peak altitude in central Honshu (Underwood and Fergusson 2005), likely associated with east–west collision at 1.2 Ma (Jolivet *et al.* 1994). This may have reduced basin capacity between the Philippine Sea and the subducting Pacific plates.

There is, however, no direct evidence to verify the age of collision in the study area, and the indirect evidence (the Japan Alps) lies thousands of kilometres away from the Mariana Trench. Therefore, we prefer the hypothesis that the enhanced aridification of the inner Asian continent was responsible for the prominent change in SAR at 1.2 Ma in the south of the Mariana Trench, and that tectonic activity may have only played a negligible role.

Deep-sea erosion and the presence of the AABW during the Pleistocene

Due to relatively continuously sedimentary environment since the late Pliocene, we estimate the ages of the bottom and the top of the JL7KGC-01A core by extrapolating the two depositional rates, 83 ± 3 – 183 ± 15 cm/Ma, yielding ages of 2.92 ± 0.14 and 0.74 ± 0.03 Ma, respectively. Extrapolation of the SAR of 183 ± 15 cm/Ma to the present suggests that 134 ± 16 cm of sediments is missing, and this is attributed to a sedimentary hiatus that affected the south of the Mariana Trench since the early middle Pleistocene.

In deep-sea sediments, hiatuses may be caused by erosion as a result of intensified bottom currents or by non-deposition due to either dissolution (carbonate or silica) resulting from corrosive deep waters or lowered surface productivity (Van Andel *et al.* 1973). In the case where sediment supply is relatively constant, changes in the chemical nature and the rate of flow of bottom waters have been invoked as the primary causes of deep-sea hiatuses in pelagic sequences (Barron and Keller 1982). For instance, within and around the C–C zone, Eastern Pacific, previous studies have indicated that the sedimentary history in this region is complex and related to the AABW (Supplemental data, Figure S4) and calcite compensation depth (CCD) fluctuation (e.g. Tracer *et al.* 1971; Van Andel *et al.* 1973; Barron and Keller 1982; Ledbetter and Ciesielski 1982; Zhu *et al.* 2001; Lyle *et al.* 2002). Because the temperature of the AABW is relatively low, the oxygen and carbon dioxide content and water density are both relatively high, and this can enhance bottom erosion as well as enhance the productivity of bottom habitat biological communities. This bottom current subsequently decomposes not only calcareous shells, but siliceous ones because it is silica unsaturated (e.g. Zhu *et al.* 2001). Thereby, during periods of high-latitude cooling, the circulation of bottom waters was intensified, which would expand these corrosive waters and increase the erosion of sediments in the C–C zone, Eastern Pacific (e.g. Tracer *et al.* 1971; Van Andel *et al.* 1973; Barron and Keller 1982; Ledbetter and Ciesielski 1982; Zhu *et al.* 2001; Lyle *et al.* 2002). Similar observations can be found along another possible path of the AABW in the Indian and Southern oceans (e.g. Watkins and Kennett 1977; Keller and Barron 1983).

In a theoretical model (e.g. Talley *et al.* 2011), the AABW was split into two branches in the Southern Pacific: one flowing eastward and northeastward into the C–C zone, Eastern Pacific, and the other transporting westward and northwestward reaching the study area (Supplemental data, Figure S4). Within a possible key path of the AABW (Supplemental data, Figure S4),

the Mariana Trench is supposed to be under the influence of fractions of the AABW (Johnson 2008). Because of these observations and this hypothesis, as well as missing sediment in our sequence, we infer that the hiatus since the early middle Pleistocene in the south of the Mariana Trench could be related to the invasion or strength of the AABW. Additionally, sea-floor landslide, abyssal earthquake, and other factors might result in this sedimentary hiatus. Due to lack of evidence and observation in this area, we prefer to correlate the 134 ± 16 cm interval of missing sediment with the presence of the AABW.

Furthermore, the latest hiatus around the C–C zone, Eastern Pacific, occurred between 2.5 and 1.0 Ma (e.g. Barron and Keller 1982; Tracer *et al.* 1971; Van Andel *et al.* 1973; Ledbetter and Ciesielski 1982; Lyle *et al.* 2002), which was much earlier than the one recorded in the south of the Mariana Trench. The end of the hiatus in the C–C zone at ~ 1 Ma possibly suggests that the AABW weakened in the Eastern Pacific, meanwhile synchronously enhanced in or expanded into the northwest Pacific since the early middle Pleistocene.

No major ice sheets existed in the Arctic area up to 2.75 Ma, after which only small ice sheets developed, and since 0.9 Ma, large ice sheets grew in both the Arctic and Antarctic areas (Raymo 1994). Chinese loess deposits from ~ 22 Ma (Guo *et al.* 2002) are useful indicators of the Arctic ice sheet variation (e.g. Hao *et al.* 2012). When the Arctic ice sheet enlarged, Asian aridification enhanced, and loess deposition accelerated, which resulted in an increase in SAR in the south of the Mariana Trench. In our record, the depositional rate change (~ 1.2 Ma) was followed by the sedimentary hiatus (~ 0.8 Ma) (Figure 6), demonstrating somewhat temporal consistence between fluctuations of the Arctic ice sheet and the AABW. Although there is no direct and reported evidence of the Arctic ice sheet influencing the AABW evolution, we will focus on this possible teleconnection between the AABW and Arctic ice sheet within the early and middle Pleistocene, by obtaining more cores, additional geochronological data as well as numerical modelling in future studies.

Conclusions

High-resolution magnetostratigraphy coupled with rock magnetic investigations have been conducted on sediment core JL7KGC-01A from the south of the Mariana Trench. The new magnetostratigraphic results indicate that the sedimentary core records chrons from the late Gauss to the early Brunhes. Thus, the sedimentary core was deposited during the

Plio-Pleistocene period. A prominent depositional hiatus is then inferred to have occurred since the early middle Pleistocene in the study area. After comparing with previous studies, we further infer that the AABW weakened in the Eastern Pacific Ocean and then enhanced or expanded westward into the south of the Mariana Trench. However, further study on this area and multiple chronologies, as well as numerical modelling, will be necessary in the future to test this inference.

Acknowledgements

The authors thank Prof. Robert J. Stern (Editor in Chief), Prof. John W. Geissman (reviewer), and one anonymous reviewer for their suggestion and comments in improving this manuscript. The authors also thank the captain and crew on the DY125-27 cruise in R/V HAI YANG LIU HAO and Dr Zhongshi Zhang in Bjerknes Centre for Climate Research for discussion.

Disclosure statement

No potential conflict of interest was reported by the authors.

Funding

This research was supported by the China Geological Survey Programme [FZH201100303], the National Natural Science Foundation of China [41402153, 40925012], the National Key Basic Research Programme of China [2012CB821900], and the Strategic Priority Research Programme of CAS [XDB06020101].

Supplemental data

Supplemental data for this article can be accessed at <http://dx.doi.org/10.1080/00206814.2015.1055597>.

References

- Asahara, Y., Tanaka, T., Kamioka, H., Nishimura, A., and Yamazaki, T., 1999, Provenance of the north Pacific sediments and process of source material transport as derived from Rb–Sr isotopic systematics: *Chemical Geology*, v. 158, p. 271–291. doi:10.1016/S0009-2541(99)00056-X
- Barron, J.A., and Keller, G., 1982, Widespread Miocene deep-sea hiatuses: Coincidence with periods of global cooling: *Geology*, v. 10, p. 577–581. doi:10.1130/0091-7613(1982)10<577:wmdhcv>2.0.co;2
- Egli, R., 2003, Analysis of the field dependence of remanent magnetization curves: *Journal of Geophysical Research: Solid Earth*, v. 108, p. 2081. doi:10.1029/2002jb002023
- Fryer, P., Becker, N., Applegate, B., Martinez, F., Edwards, M., and Fryer, G., 2003, Why is the challenger deep so deep? *Earth and Planetary Science Letters*, v. 211, p. 259–269. doi:10.1016/S0012-821X(03)00202-4
- Gordon, A.L., Huber, B., McKee, D., and Visbeck, M., 2010, A seasonal cycle in the export of bottom water from the

- Weddell Sea: *Nature Geosciences*, v. 3, p. 551–556. doi:10.1038/ngeo916
- Gordon, A.L., Orsi, A.H., Muench, R., Huber, B.A., Zambianchi, E., and Visbeck, M., 2009, Western Ross Sea continental slope gravity currents: *Deep Sea Research Part II: Topical Studies in Oceanography*, v. 56, p. 796–817. doi:10.1016/j.dsr2.2008.10.037
- Greaves, M.J., Elderfield, H., and Sholkovitz, E.R., 1999, Aeolian sources of rare earth elements to the Western Pacific Ocean: *Marine Chemistry*, v. 68, p. 31–38. doi:10.1016/S0304-4203(99)00063-8
- Guo, Z.T., Ruddiman, W.F., Hao, Q.Z., Wu, H.B., Qiao, Y.S., Zhu, R.X., Peng, S.Z., Wei, J.J., Yuan, B.Y., and Liu, T.S., 2002, Onset of Asian desertification by 22 Myr ago inferred from loess deposits in China: *Nature*, v. 416, p. 159–163. doi:10.1038/416159a
- Hao, Q., Wang, L., Oldfield, F., Peng, S., Qin, L., Song, Y., Xu, B., Qiao, Y., Bloemendal, J., and Guo, Z., 2012, Delayed build-up of Arctic ice sheets during 400,000-year minima in insolation variability: *Nature*, v. 490, p. 393–396. doi:10.1038/nature11493
- Hilgen, F.J., Lourens, L.J., and Van Dam, J.A., 2012, The Neogene period, in Gradstein, F.M., Ogg, J.G., Schmitz, M. D., and Ogg, G.M., eds., *The geological time scale 2012*: Boston, MA, Elsevier BV, p. 923–978.
- Huang, T.C., and Watkins, N.D., 1977, Contrasts between the Brunhes and Matuyama sedimentary records of bottom water activity in the South Pacific: *Marine Geology*, v. 23, p. 113–132. doi:10.1016/0025-3227(77)90085-8
- Hussong, D.M., and Uyeda, S., 1981, Tectonic processes and the history of the Mariana Arc: A synthesis of the results of Deep Sea Drilling Project Leg 60, Initial Reports of the Deep Sea Drilling Project, p. 909–929.
- Jackson, M., Worm, H.-U., and Banerjee, S.K., 1990, Fourier analysis of digital hysteresis data: Rock magnetic applications: *Physics of the Earth and Planetary Interiors*, v. 65, p. 78–87. doi:10.1016/0031-9201(90)90077-B
- Jacobs, S.S., Amos, A.F., and Bruchhausen, P.M., 1970, Ross sea oceanography and antarctic bottom water formation: *Deep Sea Research and Oceanographic Abstracts*, v. 17, p. 935–962. doi:10.1016/0011-7471(70)90046-X
- Johnson, G.C., 2008, Quantifying Antarctic bottom water and north Atlantic deep water volumes: *Journal of Geophysical Research: Oceans*, v. 113, p. C05027. doi:10.1029/2007jc004477
- Jolivet, L., Tamaki, K., and Fournier, M., 1994, Japan Sea, opening history and mechanism: A synthesis: *Journal of Geophysical Research: Solid Earth*, v. 99, p. 22237–22259. doi:10.1029/93jb03463
- Jurdy, D.M., 1979, Relative plate motions and the formation of marginal basins: *Journal of Geophysical Research: Solid Earth*, v. 84, p. 6796–6802. doi:10.1029/JB084iB12p06796
- Keller, G., and Barron, J.A., 1983, Paleooceanographic implications of Miocene deep-sea hiatuses: *Geological Society of America Bulletin*, v. 94, p. 590–613. doi:10.1130/0016-7606(1983)94<590:piomdh>2.0.co;2
- Kennett, J.P., and Watkins, N.D., 1975, Deep-sea erosion and manganese nodule development in the Southeast Indian Ocean: *Science*, v. 188, p. 1011–1013. doi:10.1126/science.188.4192.1011

- Kirschvink, J.L., 1980, The least-squares line and plane and the analysis of palaeomagnetic data: *Geophysical Journal International*, v. 62, p. 699–718. doi:10.1111/j.1365-246X.1980.tb02601.x
- Kruiver, P.P., Dekkers, M.J., and Heslop, D., 2001, Quantification of magnetic coercivity components by the analysis of acquisition curves of isothermal remanent magnetisation: *Earth and Planetary Science Letters*, v. 189, p. 269–276. doi:10.1016/S0012-821X(01)00367-3
- Ledbetter, M.T., and Ciesielski, P.F., 1982, Bottom-current erosion along a traverse in the South Atlantic sector of the Southern Ocean: *Marine Geology*, v. 46, p. 329–341. doi:10.1016/0025-3227(82)90087-1
- Lyle, M.W., Wilson, P.A., Janecek, T.R., Backman, J., Busch, W.H., Coxall, H.K., Faul, K., Gaillot, P., Hovan, S.A., Knoop, P., Kruse, S., Lanci, L., Lear, C., Moore, T.C., Nigrini, C.A., Nishi, H., Nomura, R., Norris, R.D., Pälike, H., Parés, J.M., Quintin, L., Raffi, I., Rea, B.R., Rea, D.K., Steiger, T.H., Tripathi, A., Berg, M. D.V., and Wade, B., 2002, Paleogene Equatorial Transect: covering Leg 199 of the Cruises of the Drilling Vessel JOIDES Resolution, Honolulu, Hawaii, to Honolulu, Hawaii, Sites 1215-1222, Proceedings of the Ocean Drilling Program, Initial Reports Volume 199.
- Marshall, J., and Speer, K., 2012, Closure of the meridional overturning circulation through Southern Ocean upwelling: *Nature Geosciences*, v. 5, p. 171–180. doi:10.1038/ngeo1391
- Ogg, J.G., and Smith, A.G., 2004, The geomagnetic polarity time scale, in Gradstein, F.M., Ogg, J.G., and Smith, A.G., eds., *Geological Time Scale 2004*: Cambridge, Cambridge University Press, p. 63–86.
- Ohshima, K.I., Fukamachi, Y., Williams, G.D., Nihashi, S., Roquet, F., Kitade, Y., Tamura, T., Hirano, D., Herraiz-Borreguero, L., Field, I., Hindell, M., Aoki, S., and Wakatsuchi, M., 2013, Antarctic Bottom Water production by intense sea-ice formation in the Cape Darnley polynya: *Nature Geosciences*, v. 6, p. 235–240. doi:10.1038/ngeo1738
- Ranken, B., Cardwell, R.K., and Karig, D.E., 1984, Kinematics of the Philippine Sea Plate: *Tectonics*, v. 3, p. 555–575. doi:10.1029/TC003i005p00555
- Raymo, M.E., 1994, The initiation of northern hemisphere glaciation: *Annual Review of Earth and Planetary Sciences*, v. 22, p. 353–383. doi:10.1146/annurev.ea.22.050194.002033
- Rea, D.K., 1994, The paleoclimatic record provided by eolian deposition in the deep sea: The geologic history of wind: *Reviews of Geophysics*, v. 32, p. 159–195. doi:10.1029/93rg03257
- Robertson, D.J., and France, D.E., 1994, Discrimination of remanence-carrying minerals in mixtures, using isothermal remanent magnetisation acquisition curves: *Physics of the Earth and Planetary Interiors*, v. 82, p. 223–234. doi:10.1016/0031-9201(94)90074-4
- Sun, J., and Liu, T., 2000, Stratigraphic evidence for the uplift of the Tibetan plateau between ~1.1 and ~0.9 myr Ago: *Quaternary Research*, v. 54, p. 309–320. doi:10.1006/qres.2000.2170
- Sun, Y., and An, Z., 2005, Late Pliocene-Pleistocene changes in mass accumulation rates of eolian deposits on the central Chinese Loess Plateau: *Journal of Geophysical Research: Atmospheres*, v. 110, p. D23101. doi:10.1029/2005jd006064
- Takebe, M., 2005, Carriers of rare earth elements in Pacific deep-sea sediments: *The Journal of Geology*, v. 113, p. 201–215. doi:10.1086/jg.2005.113.issue-2
- Talley, L.D., Pickard, G.L., Emery, W.J., and Swift, J.H., 2011, *Descriptive physical oceanography* (sixth edition): Boston, Academic Press.
- Tauxe, L., 2010, *Essentials of Paleomagnetism*: Berkeley, University of California Press.
- Tauxe, L., Mullender, T.A.T., and Pick, T., 1996, Potbellies, wasp-waists, and superparamagnetism in magnetic hysteresis: *Journal of Geophysical Research: Solid Earth*, v. 101, p. 571–583. doi:10.1029/95jb03041
- Tracer, J.I., Sutton, G.H., Nesteroff, W.D., Galehouse, J., Borch, C. C.V.D., Moore, T.C., Bilal UI Haq, U.Z., and Beckmann, J.P., 1971, Site Reports, Site 69, Deep Sea Drilling Project, DSDP Volume VIII, p. 61–134.
- Underwood, M.B., and Fergusson, C.L., 2005, Late Cenozoic evolution of the Nankai trench-slope system: Evidence from sand petrography and clay mineralogy: *Geological Society, London, Special Publications*, v. 244, p. 113–129. doi:10.1144/gsl.sp.2005.244.01.07
- Van Andel, T.H., Heath, G.R., Bennett, R.H., Bukry, J.D., Charleston, S., Cronan, D.S., Dinkelman, M.G., Kaneps, A.G., Rodolfo, K.S., and Yeats, R.S., 1973, Shipboard Site Reports, Site 163, Deep Sea Drilling Project, DSDP Volume XVI, p. 411–471.
- Watkins, N.D., and Kennett, J.P., 1977, Erosion of deep-sea sediments in the Southern Ocean between longitudes 70° E and 190°E and contrasts in manganese nodule development: *Marine Geology*, v. 23, p. 103–111. doi:10.1016/0025-3227(77)90084-6
- Whitworth, T., and Orsi, A.H., 2006, Antarctic Bottom Water production and export by tides in the Ross Sea: *Geophysical Research Letters*, v. 33, p. L12609. doi:10.1029/2006gl026357
- Zhu, K., Li, Z., and He, G., 2001, *The mineral resources of polymetallic nodules in the Eastern Pacific Ocean*: Beijing, Geological Publishing House.
- Zijderveld, J.D.A., 1967, Demagnetization of rocks: Analysis of results, in Collinson, D.W., Creer, K.M., and Runco, S.K., eds., *Methods in paleomagnetism*: New York, Elsevier, p. 254–286.